Effect of Multiwalled Carbon Nanotubes on Crystallization Behavior of Poly(vinylidene fluoride) in Different Solvents

Linghao He,[1,2] Jing Sun,[2] Xiaoli Zheng,[1] Qun Xu,[1] Rui Song[2,3]

[1]*College of Materials Science and Engineering, Zhengzhou University, Zhengzhou 450052, People's Republic of China*
[2]*Henan Provincial Key Laboratory of Surface and Interface Science, Zhengzhou University of Light Industry, Zhengzhou 450052, People's Republic of China*
[3]*College of Chemistry and Chemical Engineering, Graduate University of Chinese Academy of Sciences, Beijing 100049, People's Republic of China*

Received 22 March 2010; accepted 1 June 2010
DOI 10.1002/app.32907
Published online 23 August 2010 in Wiley Online Library (wileyonlinelibrary.com).

ABSTRACT: In this study, the poly(vinylidene fluoride) (PVDF)—multiwalled carbon nanotubes (MWNTs) composites have been prepared by solution casting in two different solvents: dimethyl sulfoxide (DMSO) and dimethylacetamide (DMAc). Fourier transform infrared spectroscopy (FTIR) and differential scanning calorimeter (DSC) results showed that the crystal phases of PVDF are quite different in the two solvents. When DMSO is used as the solvent, the PVDF crystalline phases could be greatly alternated from α-form to β-form by the incorporation of MWNTs. While the crystalline structure of PVDF hardly change in the case of DMAc. The DSC and polarized optical microphotographs implied that MWNTs not only act as nucleating agents for PVDF but also confine the crystallization of PVDF. Besides, it was found that the storage modulus (E') of the composites were significantly enhanced with an appropriate content of MWNTs. And when using DMSO as the solvent, one relaxation process emerges in the loss tan δ (loss factor) curves of the neat PVDF and PVDF/MWNTs composites, while it was not observed in the DMAc system. The obtained results revealed that varing solvents have different effects on the crystallization behavior of PVDF with the addition of MWNTs. © 2010 Wiley Periodicals, Inc. J Appl Polym Sci 119: 1905–1913, 2011

Key words: PVDF; MWNTs; composite

INTRODUCTION

Fluorinated polymers have a broad spectrum of applications. A well-known polymer in this family is poly(vinylidene fluoride) (PVDF).[1] This polymer has attracted much attention due to its chemical resistance, abrasion resistance, radiation resistance, mechanical strength, and piezoelectric properties. And it has been widely used in diverse fields such as transducers for sensitive scientific instruments and pipes for caustic chemical byproducts.[2–4] Especially, PVDF has been exploited in the development of electronic devices owing to its piezoelectric and pyroelectric characteristics originated from a typical crystal polymorph, β-phase.[5] In fact, PVDF can exist in five distinct crystal polymorphs depending on the crystallization condition, so-called nonpolar α-phase, polar β- and γ-phase, δ and ε.[4,6] The different crystal phases are associated with the varying polymer properties. The β-phase has an all-trans conformation (TTTT) comprising fluorine atoms and hydrogen atoms on opposite sides of the polymer backbone, resulting in a net non-zero dipole moment. The polymorph makes the β-phase become the most polar phase among the five crystals, and it has been used extensively in piezoelectric, pyroelectric, and ferroelectric applications.[7]

A variety of experimental techniques have been developed to induce β-phase formation. The polar β-phase in PVDF has been normally obtained by uniaxial or biaxial drawing of α-phase films, and simultaneous stretching, quenching, and poling of the film.[8,9] Other methods for obtaining β-phase have also been proposed.[10–12] Typically, supercritical carbon dioxide (SC CO2) method,[13] electrospinning technique,[14,15] and strong electric field[16] have also been explored. In addition, the incorporation of nanoparticles into PVDF could also influence the crystallization of PVDF in that PVDF chains are confined by the dispersed nanoparticles, then resulting in different crystallization behaviors and structures. The PVDF composites containing SiO_2,[17–20] carbon

Correspondence to: Q. Xu (qunxu@zzu.edu.cn) or R. Song (rsong@gucas.ac.cn).
Contract grant sponsor: National Natural Science Foundation of China; contract grant numbers: 20974102, 20804040, 50955010.
Contract grant sponsor: Program for New Century Excellent Talents in University (NCET).

nanotubes (CNTs),[21] clay,[22–25] acrylic rubber,[26] and Fe/Pd nanoparticle [27] have been studied.

Due to the special characters as high aspect ratios, extraordinary mechanical strength, high electrical, and thermal conductivity, CNTs have been expected as attractive fillers for polymer matrixes to achieve high performance and multifunctions.[28–31] Specified to PVDF/CNT systems, their preparation and physical characterization have been explored recently. And various fabricated methods such as ultrahigh-shear processing approach and melt-compounding technique have been used.[32,33] The enhancement of the piezoelectric β-polymorph of the nanocomposites in solution-cast films of PVDF and PVDF-based copolymers through blending them with CNTs using the *N*,*N*-dimethylacetamide as solvent was first reported by Carroll's group.[34] In our previous studies, we reported the effect of multiwalled carbon nanotubes on the crystallization behavior of PVDF when *N*,*N*-dimethylformamide was used as solvent.[35] As reported, the crystallization behavior of the crystalline polymer could be obviously affected by the cast solvents.[7,36,37] Hence, in this work, we focus on the effect of different solvents (dimethyl sulfoxide and *N*,*N*-dimethylacetamide) on the crystalline, thermal, and dynamic mechanical behaviors of PVDF with the presence of MWNTs.

EXPERIMENTAL

Materials

PVDF powders were purchased from Resin Corp. of Changzhou, China (F401, $M_n = 150 \times 10^3$, determined from the GPC measurement) and used as received. Multiwalled carbon nanotubes (MWNTs) were purchased from Shenzhen Nanotech Port Co. with ca. 10–20 nm in diameter and 5–15 micrometers in length. They were purified with 2.4 *M* nitric acid for 0.5 h. The resulting MWNTs were then centrifuged, collected, and dried in a vacuum oven. Dimethyl sulfoxide (DMSO) was purchased from Sinopharm Chemical Reagent Co. (China). Dimethylacetamide (DMAc) was purchased from Tianjin Chemical Reagent Company (China).

Preparation of PVDF/MWNTs composites

PVDF was dissolved in 20 mL solvent by stirring for 3 h. A various amount of purified MWNTs were dispersed in 10 mL solvent by mild sonication in an ultrasonic cleaning bath for 3 h to generate a suspension. The MWNTs suspension was dropwisely added to the PVDF matrix solutions while stirring. And then, the mixture was stirred for another 3 h (mass ratio of PVDF = 1 wt %). Then the films were obtained by pouring the mixture into a Petri dish. Finally the resultants were annealed under vacuum at 120°C for 12 h to form homogeneous films. The blends of PVDF/MWNTs were prepared in different composition ratios (w/w) of 0.1, 0.2, 0.3, 0.4, 0.5 wt %, respectively. Control samples of the pure PVDF matrix formulations were prepared in a similar fashion, using pure solvent to replace the MWNTs suspensions and to maintain the same overall solvent volume. To obtain more insight on the morphologic structures by polarizing microscope, approximately 1 mL of the mixture was added in self-made aluminum cell (2×2 cm^2) followed by annealed under vacuum at 120°C for 12 h.

Measurement and characterization

Fourier transform infrared (FTIR) spectra were recorded on a Bruker Tensor 27 FTIR spectrophotometer using attenuated total reflection (ATR) model, at the resolution of 2 cm^{-1}, 32 scans. Crystallization studies were conducted by means of differential scanning calorimetery (DSC Q100, TA Instruments) which equipped with the thermal analysis data system. A continuous nitrogen flow (50 mL/min) in the DSC sample cell was maintained. The samples were analyzed between room temperature and 200°C at a heating or cooling rate of 10°C/min under a nitrogen atmosphere. Dynamic mechanical analysis (DMA) was performed using a DMA Q800 (TA Instruments) at a fixed frequency of 1 Hz and a temperature sweep of 3°C per step ranging from 30°C to 160°C. Scanning electron microscope (SEM, JEOL JSM-6490LV) was used to observe the dispersion of MWNTs in composites. The dynamic storage modulus (E') and damping tangent (tan δ) curves against temperature were plotted. The sample dimension was $30 \times 5 \times 0.2$ mm^3. A polarized optical micrograph (POM) was obtained under crossed polarizers using a Nikon E600POL at room temperature. The photographs for the sample films were taken with a Nikon Coolpix 5600 digital camera equipped on the vertical hood of the optical microscope.

RESULTS AND DISCUSSION

FTIR analysis

The infrared data of pure PVDF and composites in certain frequency ranges are showed in Figure 1. According to the previous reports,[38–40] the infrared bands at 1383, 976, 795, 764, and 615 cm^{-1} are attributed to the α-form of PVDF, while the band at 840 cm^{-1} is ascribed to the all-trans conformations of the β-form.

As is shown in Figure 1(A), when DMSO is used as the solvent, the typical absorption peaks attributed to the α- and β-forms were both observed and

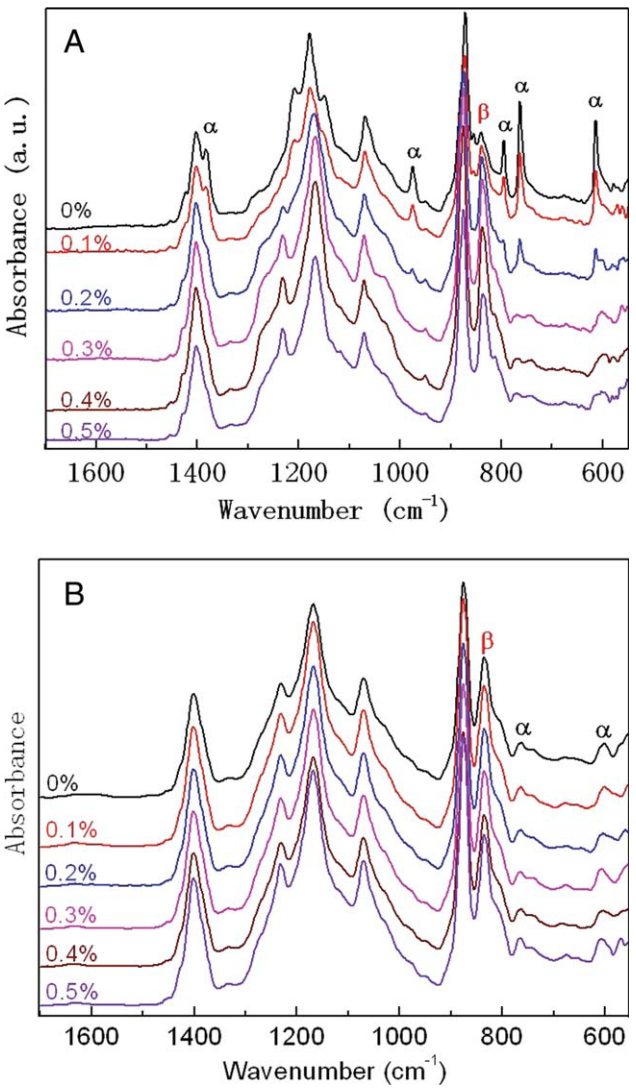

Figure 1 FTIR spectra of membranes prepared with pure PVDF and PVDF/MWNTs composites with different blending mass ratios using DMSO (A) and DMAc (B) as solvent. [Color figure can be viewed in the online issue, which is available at wileyonlinelibrary.com.]

apparently α-form is the predominant phase for the pure PVDF. After adding the MWNTs, there is a great variation in the relative intensity of the vibrational bands in comparison to the pure PVDF. Namely, with the increasing content of MWNTs, the intensity of the vibrational bands at 840 cm^{-1} ascribed to the β-form crystal is enhanced gradually. On the contrary, the intensity of the bands at 1383, 976, 795, 764, and 615 cm^{-1} ascribed to the α-form crystals are all weakened. When the content of MWNTs reaches 0.3 wt %, the effects are more pronounced and the spectra of PVDF/MWNTs composite show no significant change with the continuing increase of MWNTs. However, when DMAc is used as the solvent, the result is completely different as compared to that in DMSO system. Just as is shown in Figure 1(B), for the pure PVDF, the typical absorption peaks attributed to the α- and β-forms also can be observed, but β-form is the predominant phase. With the increasing content of MWNTs, the intensity of all the bands hardly change. In fact, the solubility parameter of PVDF is 23.2 $(J/cm^3)^{1/2}$, which is closer to that of DMAc (22.7) than that of DMSO (27.4).[41,42] Due to the good dissolving power of DMAc to PVDF, PVDF chains can fully extend in DMAc and thus be favorable to form flat-serrated crystals, i.e., molecular chains exist in the form of β-phase along the stem of MWNTs. So it is evident that choosing proper solvent can help to obtain the desired crystal, which is closely interrelated to the properties of materials.

Based on the specific absorption bands of α- and β- phase, a method used to calculate the fraction of β-phase had been introduced.[43] The fraction of β-phase, $F(\beta)$, can be calculated using the following equation [44]:

$$F(\beta) = A_\beta/(1.26\ A_\alpha + A_\beta) \quad (1)$$

where A_α and A_β are the absorbencies of α- and β- phase at 763 cm^{-1} and 840 cm^{-1}, respectively, and the $F(\beta)$ values derived from the FTIR test are listed in Table I.

As is shown in Table I, when DMSO is used as solvent, the $F(\beta)$ value of pure PVDF is the lowest (33.1%), which implies that α-form is the predominant phase. With the increasing content of MWNTs, the $F(\beta)$ value becomes higher and reaches 73.9%, when the content of MWNTs is 0.5 wt %. These results reveal that incorporation of MWNTs facilitates the formation of β-phase crystals in DMSO. In the case of DMAc system, the $F(\beta)$ value of 65.8% for the pure PVDF is much higher than that in DMSO. However, the $F(\beta)$ value almost remain unchanged with the incorporation of MWNTs in DMAc.

Thermal behaviors

DSC measurements are performed to investigate the thermal behavior of the samples. DSC heating and

TABLE I
***F*(β) Values of Samples**

Sample	PVDF	0.1%	0.2%	0.3%	0.4%	0.5%
DMSO-*F*(β) (%)	33.1	44.3	59.6	71.5	73.3	73.9
DMAc-*F*(β) (%)	65.8	68.2	68.1	68.7	67.9	68.1

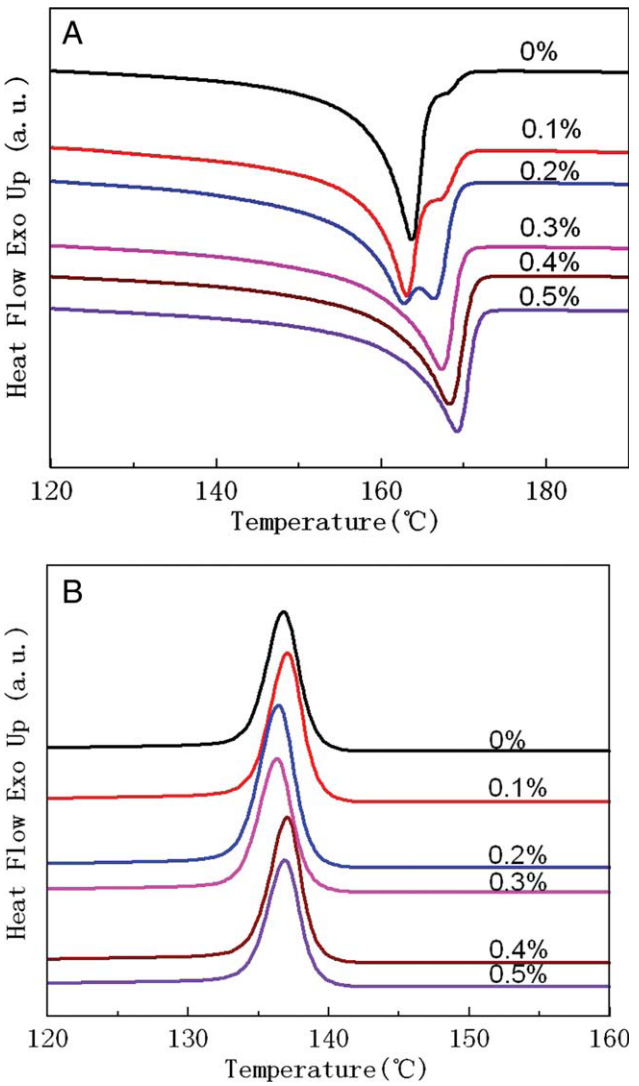

Figure 2 DSC heating (A) and cooling (B) curves of the pure PVDF and PVDF/MWNTs composites using DMSO as solvent. [Color figure can be viewed in the online issue, which is available at wileyonlinelibrary.com.]

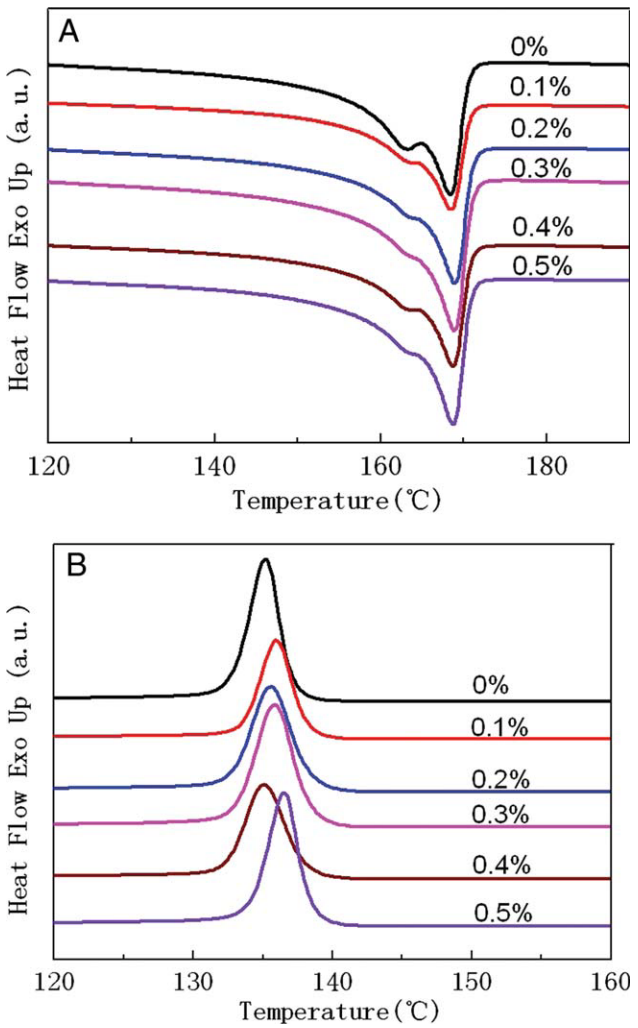

Figure 3 DSC heating (A) and cooling (B) curves of the pure PVDF and PVDF/MWNTs composites using DMAc as solvent. [Color figure can be viewed in the online issue, which is available at wileyonlinelibrary.com.]

cooling curves of PVDF and composite films were presented in Figures 2 and 3, and the corresponding data are summarized in Tables II and III. When DMSO is used as the solvent, it can be found that one main melting peak appears at 163°C and one shoulder peak locates at around 168°C for the pure PVDF [Fig. 2(A)]. With an increase of the MWNTs content, the shoulder peak becomes powerful. When the content of MWNTs is 0.5 wt %, one melting peak can be observed. The double melting endotherm arises either due to melting-recrystallizing phenomenon or the presence of two different types of crystal structures.[45,46] Andrew et al.[15] studied the electrospun PVDF fibers and they considered that α phase has the lower melting temperature, while β-phase has the higher melting temperature, and

TABLE II
DSC Parameters of the Pure PVDF and PVDF/MWNTs Composites Using DMSO as Solvent

Sample	$T_{m,\ peak}$ (°C)	ΔH_m (J/g)	X_c (%)	$T_{c,\ onset}$ (°C)	$T_{c,\ peak}$ (°C)
0%	163.59/167.8	45.98	43.96	142.22	136.78
0.1%	163.01/167.1	49.82	47.68	142.68	137.08
0.2%	162.36/166.70	51.16	49.01	142.68	136.47
0.3%	167.29	55.28	53.01	142.22	136.29
0.4%	168.30	54.80	52.6	143.44	136.97
0.5%	169.13	53.39	51.3	143.74	136.92

TABLE III
DSC Parameters of the Pure PVDF and PVDF/MWNTs Composites Using DMAc as Solvent

Sample	$T_{m,\ peak}$ (°C)	ΔH_m (J/g)	X_c (%)	$T_{c,\ onset}$ (°C)	$T_{c,\ peak}$ (°C)
0%	162.86/168.39	56.77	54.27	141.31	135.23
0.1%	168.48	51.16	48.96	141.62	136.02
0.2%	168.96	57.70	55.27	142.83	135.54
0.3%	168.87	60.88	58.38	143.59	135.84
0.4%	168.73	52.03	49.94	143.89	135.08
0.5%	168.64	59.43	57.10	143.74	136.47

thus the endothermic peak is weighted toward higher temperature, which is indicative of the relative amount of the β-phase to α-phase in sample. Hence, with an increase of the MWNTs content, the main melting peak shifts from 163°C to 168°C suggests a MWNTs-induced PVDF crystal transformation from α-phase to β-phase, which is in agreement with FTIR results [Fig. 1(A)]. When DMAc is used as the solvent, the main melting peak appears at about 168°C whereas the shoulder peak registers near 163°C. And with an increasing of the MWNTs content, there is no shift and the relative intensity

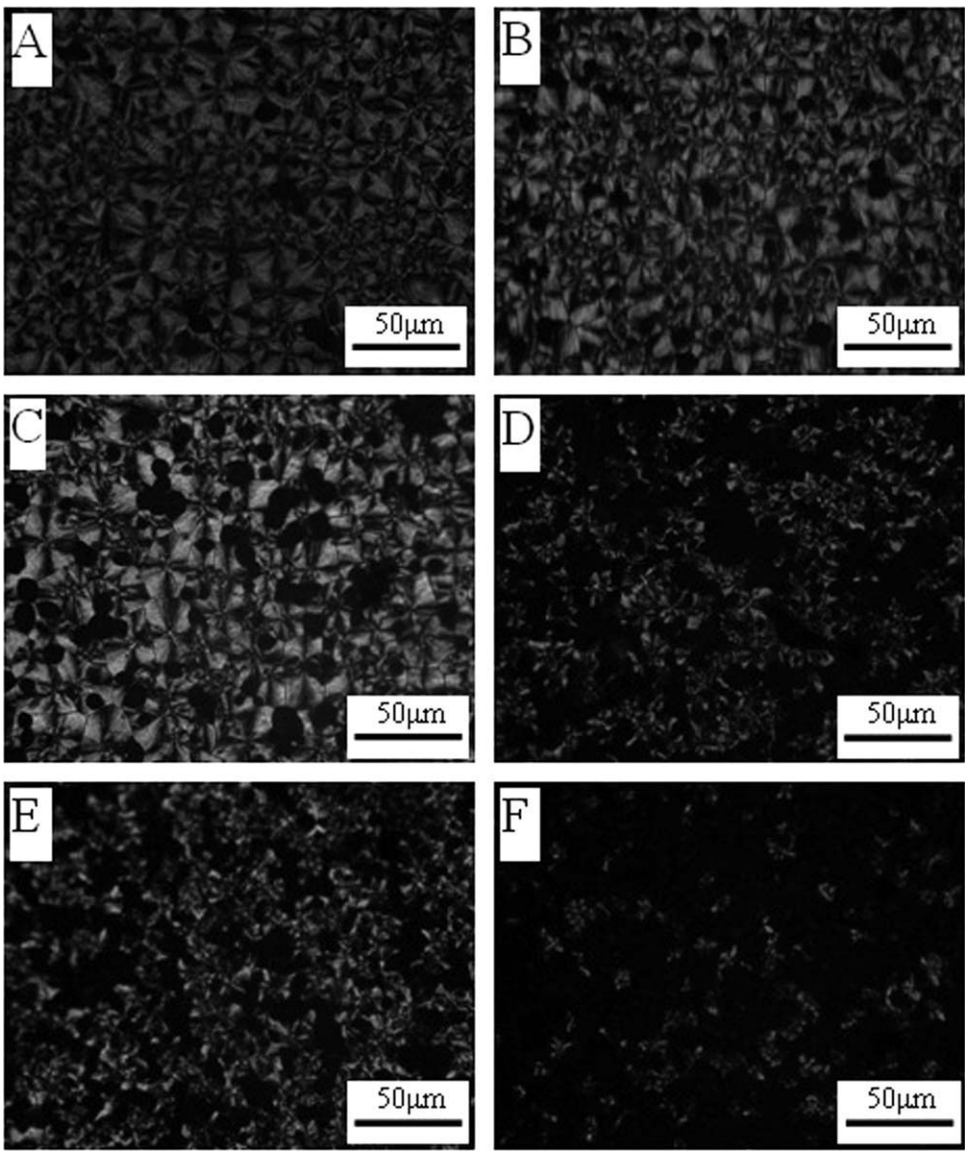

Figure 4 Polarized light macroscopic images of samples using DMSO as solvent with different MWNTs contents. (A) pure PVDF; (B) 0.1 wt % MWNTs; (C) 0.2 wt % MWNTs; (D) 0.3 wt % MWNTs; (E) 0.4 wt % MWNTs; (F) 0.5 wt % MWNTs.

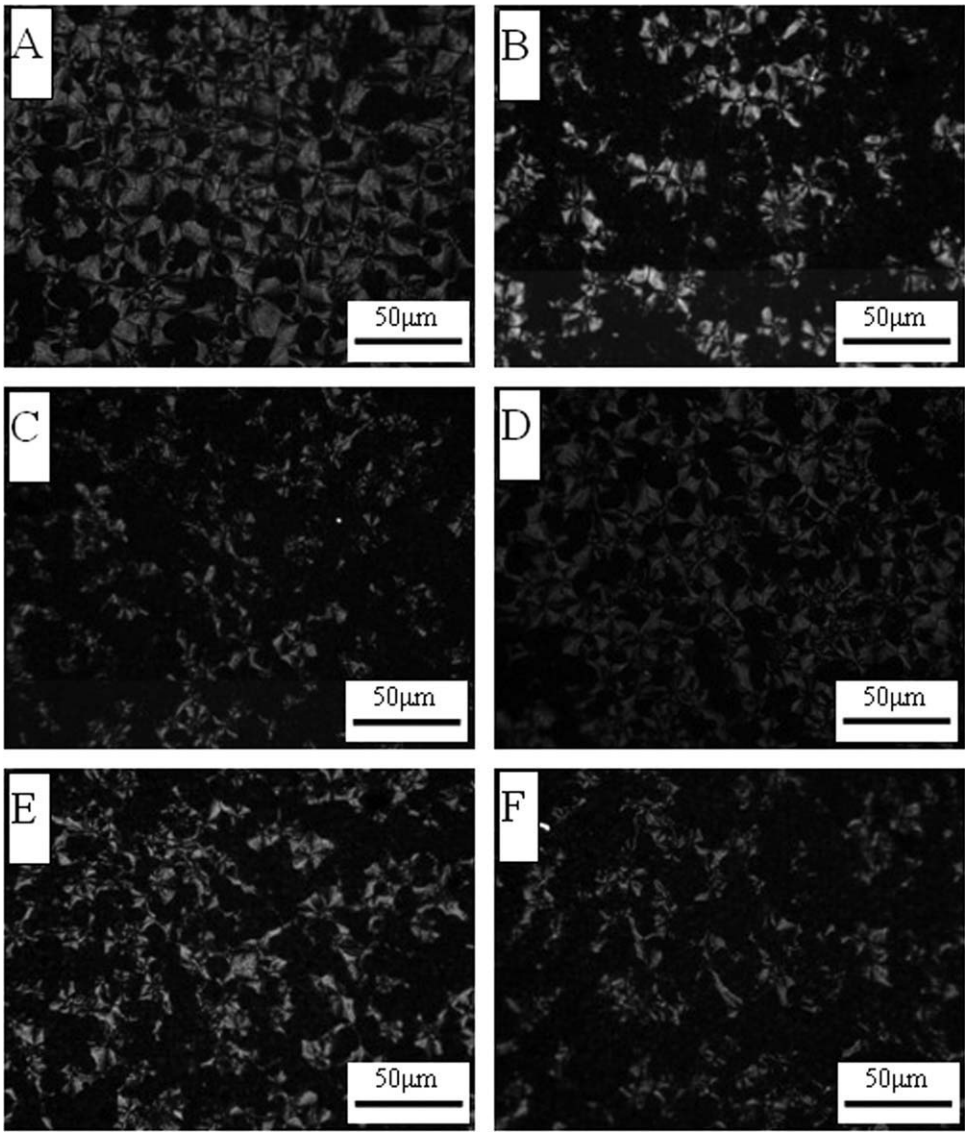

Figure 5 Polarized light macroscopic images of samples using DMAc as solvent with different MWNTs contents. (A) pure PVDF; (B) 0.1 wt % MWNTs; (C) 0.2 wt % MWNTs; (D) 0.3 wt % MWNTs; (E) 0.4 wt % MWNTs; (F) 0.5 wt % MWNTs.

hardly change. The result is consistent with the results shown in Figure 1(B).

From the DSC results, the crystallinity of the mass (x_c(%)) can be calculated from the melting enthalpy of the second heating trace (ΔH_m) with the following relation:

$$x_c(\%) = \frac{\Delta H_m}{(1-w)\Delta H_0} \quad (2)$$

where $\Delta H_0 = 104.6$ J/g is the heat of fusion for 100 % crystalline PVDF [47,48], and w is the MWNTs content in the PVDF/MWNTs composites. The corresponding data from Figures 2 and 3 are summarized in Tables II and III.

When DMSO is used as the solvent (Table II), it can be observed that the temperature of crystallization peak ($T_{c,\text{peak}}$) remain almost no change, whereas the temperature of crystallization onset ($T_{c,\text{onset}}$) increase with the addition of MWNTs due to the nucleating action of the MWNTs. Besides, the X_c apparent enhance with the increasing of MWNTs content. However, the value of X_c did not increase monotonically as the amount of MWNTs increased, but to increase first and then decrease. In the case of 0.3 wt % of MWNTs, X_c achieves the highest value compared with other composite samples. The results suggest that there exists a competition between nucleating function and confining crystallization of the inorganic MWNTs. Indeed, in the polymer-inorganic hybrids comprising a crystalline polymer and a crosslinked inorganic network, the polymer could crystallize in different ways. On one hand, when the content of the inorganic component lies in a low

range, it could act as a nucleating agent for crystallization to facilitate the crystallization process. On the other hand, with a further increasing the inorganic component, there is a possibility that excessive inorganic may form an inorganic network, which could restrict the polymer in a micro-environment surrounded by the inorganic component. Therefore, the crystallization of polymer and the crystallization kinetics could be confined. When DMAc is used as the solvent, the variational trend of $T_{c,\text{onset}}$ and X_c is similar to those in DMSO system.

To corroborate the above DSC results, POM is used to further observe the crystalline structure of PVDF and composite films.

Polarized optical microscopy

The POM images in Figures 4 and 5 provide evidence that supports the effectiveness of the MWNTs as a nucleating agent. It can be seen from Figure 4(A) that the pure PVDF in DMSO shows strongly birefringent α-phase spherulites with the uniform size, averaging about 30 μm in diameter. With the addition of the MWNTs, on one hand, the number of the spherulites increases significantly as evident from the Figure 4(B–E); on the other hand, the spherulites size decreases drastically so that there are no measurable dimensions of the spherulites with the MWNTs content of more than 0.3 wt %. In fact, if the density of nuclei is high, it will be difficult to develop the whole spherulites since the nuclei are too close to each other to allow free growth. When DMAc is used as the solvent, the POM images of pure PVDF and the PVDF/MWNTs composites are shown in Figure 5. With the increasing content of MWNTs, a lowered spherulite size is observed, which suggests that the excessive MWNTs in the hybrid composite would disturb the crystal growth of PVDF component. Therefore, it can be concluded that the crystalline morphology of PVDF can be strongly influenced by MWNTs. Namely, MWNTs can provide nucleating sites and physical barriers for the growth of PVDF spherulites.

Fracture morphology of the composites

The fracture surfaces of PVDF/MWNTs composites using DMSO as the solvent are characterized by SEM, and two representative SEM micrographs with 0.2 wt % and 0.5 wt % MWNTs are presented in Figure 6. In Figure 6(A), the well-dispersed bright dots and lines which are the ends of the broken MWNTs has been marked by arrows. It is suggested that a homogeneous dispersion of MWNTs in the PVDF matrix is achieved when the loaded content of MWNTs is lower (0.2 wt %). Nevertheless, when the MWNTs content is higher (0.5 wt %), aggregated MWNTs can be obviously seen as is shown in Figure 6(B), which is disadvantage to improve the mechanical properties of the composite. The following will discuss this section.

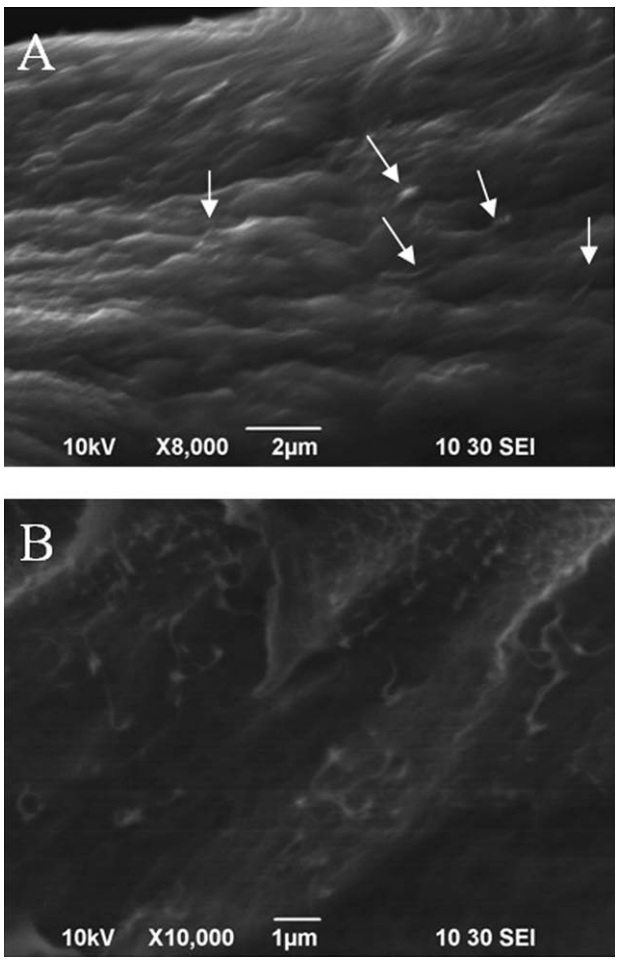

Figure 6 SEM images showing an overall morphology of a fracture surface for PVDF/MWNTs composites using DMSO as solvent with different MWNTs contents. (A) 0.2 wt % MWNTs and (B) 0.5 wt % MWNTs.

Dynamic mechanical properties

DMA measurements are employed to study the effect of MWNTs on the thermo-mechanical properties of PVDF. The storage modulus (E') as a function of temperature for PVDF and PVDF/MWNTs composites have been exhibited in Figures 7 and 8. As expected, MWNTs are effective in enhancing the E' of composites as a nanofiller. When DMSO is used as the solvent, the E' of the composite with 0.2 wt % MWNTs reaches 1386 MPa, which is 18.7% higher than that of neat PVDF. In particular, when DMAc is used as the solvent, E' increases from 770 MPa for pure PVDF to 1590 MPa for the composite with 0.3 wt % MWNTs, representing 106.5% improvement. Nevertheless, the values of E' do not increase monotonically with the increase of MWNTs content, and

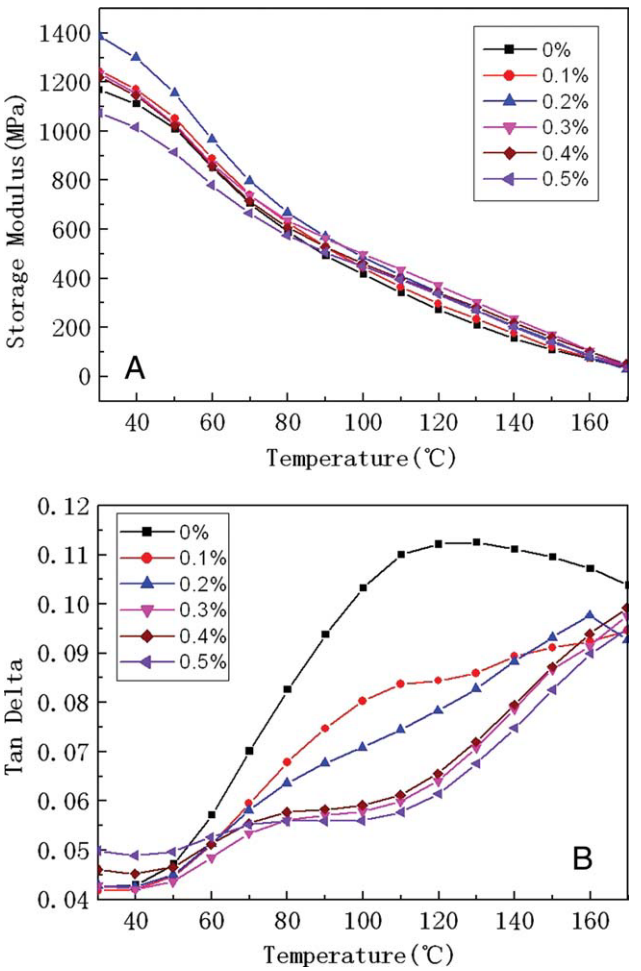

Figure 7 Temperature dependence of storage modulus (A) and tan δ (B) of pure PVDF and PVDF/MWNTs composites using DMSO as solvent. [Color figure can be viewed in the online issue, which is available at wileyonlinelibrary.com.]

there exists an inclination that the value of E' first increases and then decreases. Generally, the higher aspect ratio of the inorganic particles corresponds to the higher surface energy and the more effective interfacial interaction between matrix and fillers. However, when plenty of MWNTs are added into the PVDF matrix, they will aggregate severely with a poor dispersion, as is shown in Figure 6(B). Therefore, the contact area between MWNTs and PVDF matrix decreases rapidly, which leads to the decrease of E'. This phenomenon indicates that there exists an optimum content for nanofiller, at which excellent mechanical and physical properties of the composites could be achieved.

The loss tangent, tan δ, of the neat PVDF and PVDF/MWNTs composites are shown in Figures 7(B) and 8(B). It is noteworthy to point out that above ca. 60°C, one relaxation process emerges in the tan δ (loss factor) curves when using DMSO as the solvent. This process, normally labeled α_c, is closely associated with the motions within the crystalline fraction, which is resulted from the higher-T_g-relaxation. This phenomenon have been reported in a variety of flexible semi-crystalline polymers, including polyethylene, poly(methylene oxide), poly(ethylene oxide), and isotactic polypropylene.[49,50] For the neat PVDF, the relaxation peak locates at about 120°C, and it gradually shifts to low temperature with the increasing content of MWNTs. The trend is consistent with that of the content ratio of α-form to β-form in PVDF crystals. It should be noted that this relaxation is not clearly revealed as a peak in the plots for all the samples shown in Figure 8(B). And this observation is also consistent with the infrared data that MWNTs have few effect on the crystal phase of PVDF when DMAc is used as the solvent.

CONCLUSIONS

In this investigation, the PVDF/MWNTs composites were prepared by solution blending using DMSO

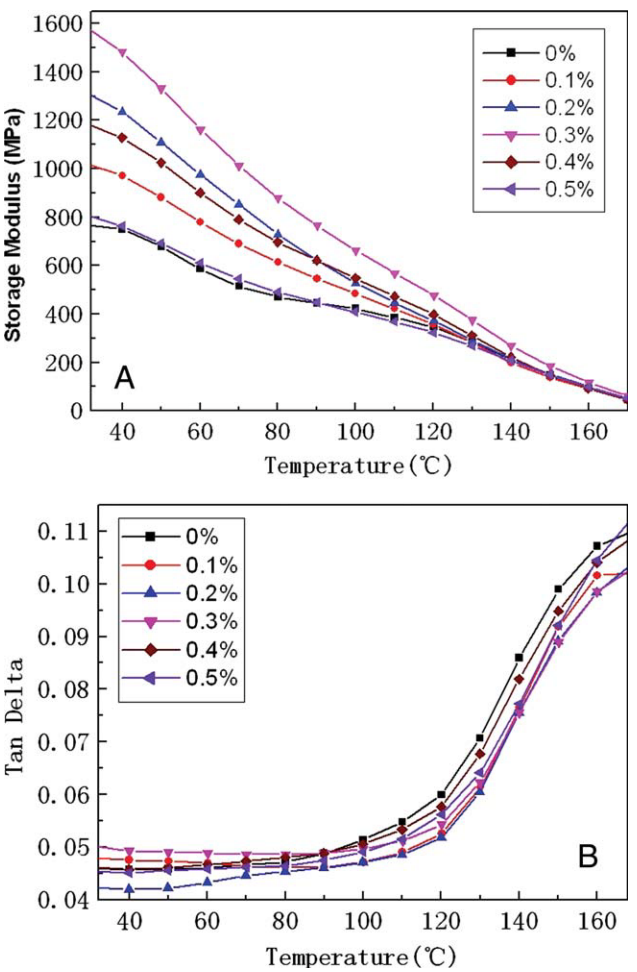

Figure 8 Temperature dependence of storage modulus (A) and tan δ (B) of pure PVDF and PVDF/MWNTs composites using DMAc as solvent. [Color figure can be viewed in the online issue, which is available at wileyonlinelibrary.com.]

and DMAc as the solvents, respectively. The effects of MWNTs content and different solvents on the crystallization behavior of composites have been studied. The FTIR measurements and the DSC results showed that the crystalline phases of PVDF are quite different in two solvents, and when DMSO is used as solvent, the crystalline phases could be greatly alternated by the incorporation of MWNTs. In addition, the DSC measurements and polarized optical microphotographs indicated that the MWNTs would not only act as nucleating agents for PVDF but also confine the crystallization of PVDF. When the content of MWNTs lies in a low range, the inorganic component could act as a nucleating agent to facilitate the crystallization process. However, with a further increasing MWNTs content, there is a possibility that excessive MWNTs may form an inorganic network, which could restrict the crystallinity and the crystalline kinetics of the polymer. In addition, it was observed that the storage modulus (E') can be significantly enhanced with the addition of MWNTs through the curve analysis of DMA. And when using DMSO as the solvent, one relaxation process can be observed in the loss tan δ curves of the neat PVDF and PVDF/MWNTs composites, while it was not observed in the DMAc system. The results revealed that varing solvents have different effects on crystallization behavior of PVDF at the presence of MWNTs.

References

1. Yang, Y.; Wu, G.; Ramalingam, S.; Hsu, S. L.; Kleiner, L.; Tang, F. Macromolecules 2007, 40, 9658.
2. Priya, L.; Jog, J. P. J Polym Sci Part B: Polym Phys 2002, 40, 1682.
3. Lang, S. B.; Muensit, S. Appl Phys A: Solids Surf 2006, 85, 125.
4. Lovinger, A. J. Science 1983, 220, 1115.
5. Kim, D.; Sun, Y.; Yun, S.; Lee, S.; Kim, B. J. Biomechanics 2005, 38, 1359.
6. Briber, R. M.; Khoury, F. J Polym Sci Part B: Polym Phys 1993, 31, 1253.
7. Park, Y. J.; Kang, Y. S.; Park, C. Eur Polym J 2005, 41, 1002.
8. Sajkiewicz, P.; Wasiak, A.; Goclowski, Z. Eur Polym J 1999, 35, 423.
9. Bergman, J. G., Jr.; McFee, J. H.; Crane, G. R. Appl Phys Lett 1971, 18, 203.
10. Lovinger, A. J. Polymer 1981, 22, 412.
11. Miller, R. J Polym Sci Polym Chem Ed 1976, 14, 2325.
12. Wang, J.; Li, H.; Lui, J.; Duan, Y.; Jiang, S.; Yan, S. J Am Chem Soc 2003, 125, 1496.
13. Imran-ul-haq, M.; Tiersch, B.; Beuermann, S. Macromolecules 2008, 41, 7453.
14. Huang, S.; Yee, W. A.; Tjiu, W. C.; Liu, Y.; Kotaki, M.; Boey, Y. C. F.; Ma, J.; Liu, T. X.; Lu, X. H. Langmuir 2008, 24, 13621.
15. Andrew, J. S.; Clarke, D. R. Langmuir 2008, 24, 670.
16. Das-Gupta, D. K.; Doughty, K. J Appl Phys 1978, 49, 4601.
17. Song, R.; Yang, D. B.; He, L. H. J Mater Sci 2007, 42, 8408.
18. Shah, D.; Maiti, P.; Gunn, E.; Schmidt, D. F.; Jiang, D. D.; Batt, C. A.; Giannelis, E. P. Adv Mater 2004, 16, 1173.
19. Kim, J. W.; Cho, W. J.; Ha, C. S. J Polym Sci Part B: Polym Phys 2002, 40, 19.
20. Buckley, J.; Cebe, P.; Cherdack, D.; Grawford, J.; Ince, B. S.; Jenkins, M.; Pan, J.; Reveley, M.; Washington, N.; Wolchover, N. Polymer 2006, 47, 2411.
21. Nam, Y. W.; Kim, W. N.; Cho, Y. H.; Chae, D. W.; Kim, G. H.; Hong, S. P.; Hwang, S. S.; Hong, S. M. Macromol Symp 2007, 249–250, 478.
22. Dillon, D. R.; Tenneti, K. K.; Li, C. Y.; Ko, F. K.; Sics, I.; Hsiao, B. S. Polymer 2005, 47, 1678.
23. Priya, L.; Jog, J. P. J Appl Polym Sci 2003, 89, 2036.
24. Qiu, Z. B.; Yan, C. Z.; Lu, J. M.; Yang, W. T. Macromolecules 2007, 40, 5047.
25. Patro, T. U.; Mhalgi, M. V.; Khakhar, D. V.; Misra, A. Polymer 2008, 49, 3486.
26. Li, Y. J.; Iwakura, Y.; Zhao, L.; Shimizu, H. Macromolecules 2008, 41, 3120.
27. Xu, J.; Bhattacharyya, D. Ind Eng Chem Res 2007, 46, 2348.
28. Oki, A.; Qiu, X. D.; Alawode, O.; Foley, B. Mater Lett 2006, 60, 2751.
29. Moniruzzaman, M.; Winey, K. I. Macromolecules 2006, 39, 5194.
30. Ajayan, P. M.; Schadler, L. S.; Giannaris, C.; Rubio, A. Adv Mater 2000, 12, 750.
31. Bose, S.; Khare, R. A.; Moldenaers, P. Polymer 2010, 51, 975.
32. Chen, G. X.; Li, Y. J.; Shimizu, H. Carbon 2007, 45, 2334.
33. Chen, D.; Wang, M.; Zhang, W. D.; Liu, T. X. J Appl Polym Sci 2009, 113, 644.
34. Levi, N.; Czerw, R.; Xing, S. Y.; Iyer, P.; Carroll, D. L. Nano Lett 2004, 4, 1267.
35. He, L. H.; Xu, Q.; Hua, C. W.; Song, R. Polym Compos 2010, 5, 921.
36. Wu, W. B.; Chiu, W. Y.; Liau, W. B. J Appl Polym Sci 1997, 64, 411.
37. Radhakrishnan, S.; Venkatachalapathy, P. D. Polymer 1996, 37, 3749.
38. Benz, M.; Euler, W. B.; Gregory, O. J. Macromolecules 2002, 35, 2682.
39. Tashiro, K.; Itoh, Y.; Kobayashi, M.; Tadokoro, H. Macromolecules 1985, 18, 2600.
40. Dikshit, A. K.; Nandi, A. K. Macromolecules 2000, 33, 2616.
41. Gao, C.; Xi, D.; Yang, X.; Meng, Y. Membr Sci Technol 2006, 26, 21.
42. He, M.; Chen, W.; Dong, X. Polymer Physics; Fu Dan University Press: Shang Hai, 2009; p 117.
43. Salimi, A.; Yousefi, A. A. Polym Test 2003, 22, 699.
44. Salimi, A.; Yousefi, A. A. J Polym Sci Part B: Polym Phys 2004, 42, 3487.
45. Phang, I. Y.; Ma, J. H.; Shen, L.; Liu, T. X.; Zhang, W. D. Polym Int 2006, 55, 71.
46. Bose, S.; Bhattacharyya, A. R.; Häuβler, L.; Pötschke, P. Polym Eng Sci 2009, 49, 1533.
47. Rosenberg, Y.; Sigmann, A.; Narkis, M.; Shkolnik, S. J Appl Polym Sci 1991, 43, 535.
48. Marega, C.; Marigo, A. Eur Polym J 2003, 39, 1713.
49. Mano, J. F.; Sencadas, V.; Mello Costa, A.; Lanceros-Méndez, S. Mater Sci Eng A 2004, 370, 336.
50. Boyd, R. H. Polymer 1985, 26, 323.